Safe and Robust Cloud-based Predictive Control for Water Distribution Networks

Kallesøe, Carsten Skovmose; Deleuran, Joakim Børlum; Balla, Krisztian Mark

Published in:
IFAC-PapersOnLine

DOI (link to publication from Publisher):
10.1016/j.ifacol.2023.10.1656

Publication date:
2023

Document Version
Publisher's PDF, also known as Version of record

Available online at www.sciencedirect.com

ScienceDirect

IFAC Papers Online CONFERENCE PAPER ARCHIVE

IFAC PapersOnLine 56-2 (2023) 749–754

Safe and Robust Cloud-based Predictive Control for Water Distribution Networks

Carsten Skovmose Kallesøe [*,**] **Joakim Børlum Deleuran** [*] **Krisztian Mark Balla** [*]

[*] *Technology Innovation, Grundfos Holding A/S, Poul Due Jensens vej 7, 8850, Bjerringbro, Denmark (e-mail: {ckallesoe,jopetersen,kballa}@grundfos.com).*

[**] *Dept. of Electronic Systems, Aalborg University, Fredrik Bajers vej 7c, 9220, Aalborg, Denmark (e-mail: csk@es.aau.dk)*

Abstract:
Water distribution networks with storage equalize the operating pressure in the system. Apart from providing pressure, elevated reservoirs also allow for exploiting fluctuation in electricity prices. In this work, we use an Economic Model Predictive Control scheme for planning the filling times of storage in water distribution networks. This controller needs access to electricity prices via an Information Technology (IT) connection to a power-trading system. Therefore, we propose a control architecture, where a Global Controller is deployed on a cloud server, whereas a locally placed data-acquisition and supervisory controller provide the safety guarantees in terms of an Operational Technology (OT) layer. The approach is demonstrated numerically on a real-world network architecture where real data is used to verify the robustness of the method.

Keywords: Drinking Water Systems, Economic Model Predictive Control, Cyber Security

1. INTRODUCTION

Electrical energy prices have dramatically increased and become volatile (International Energy Agency (2022)) in many parts of the world, and there is a general trend of pushing towards the use of electrical power produced from renewables. In fact, it is expected that the correlation between the price and the availability of renewable energy will increase in the coming decades. Energy systems with some type of storage can harvest this price volatility, that not only results in operational expenditure savings but also cleaner energy use. Elevated reservoirs represent energy storage in water distribution networks, having a good foundation for exploiting energy price volatility.

Energy prices are negotiated on the day-ahead energy market and are publicly available via Information Technology (IT) platforms in several countries around the world (ENTSO (2022)). Access to these prices enables optimizing pump operation in water networks. However, this requires a control architecture that combines IT and hardware needs regarding control, instrumentation, and communication also called Operating Technology (OT). As a consequence of integrating IT and OT, the risk of physical harm due to cyber-attacks is increased significantly. Nevertheless, the benefits of integrating IT/OT for water networks are substantial and therefore should be pursued.

In this paper, the control of water distribution networks with elevated reservoirs is considered. Scheduling storage filling using optimal control methods has been investigated extensively, e.g., in Cembrano et al. (2000), Trnka et al. (2011), Ocampo-Martinez et al. (2013), Wang et al. (2017), whereas an early review is given in Corte and Sörensen (2013). Cyber-security in water networks is considered in Rao and Francis (2015) and possible ways improving security in Rao and Francis (2015), Taormina et al. (2019) and Douglas et al. (2019). Cyber-security has a great impact in practice, yet it is an unresolved issue when it comes to combining IT/OT for control of water networks.

The control architecture proposed in this work has the optimization problem placed on a cloud server, where IT access is provided to day-head electrical price data through a third-party interface. Locally, at the pumping stations, controllers are gathering data and executing control actions. The local controllers are developed as safety filters, thereby protecting the system against different failures, cyber-attacks, and unexpected network events. This split between cloud and local control software is chosen to lower the computational load at the local controllers, and thereby enable to use less expensive controller hardware. In Escudero et al. (2018) the idea of introducing safety filters for cyber-security is proposed in an industrial IT/OT context. Safety filters are also used for safe Reinforcement Learning control of water network in Val et al. (2021).

To justify the need for easy commissionable and cyber-secure control architectures for water distribution networks, we introduce first the network dynamics in Section 2. Then, we present the proposed methods in Section 3. The benefits are exemplified in a numerical study in Section 4. Finally, we provide some concluding remarks.

2. PRELIMINARIES - SYSTEM DESCRIPTION

We consider a water distribution network (or part of a network) with a structure depicted in Fig. 1.

⋆ This work was supported by the CRUCIAL project, funded by Innovation Fund Denmark, grant number 1063-00001B.

10.1016/j.ifacol.2023.10.1656

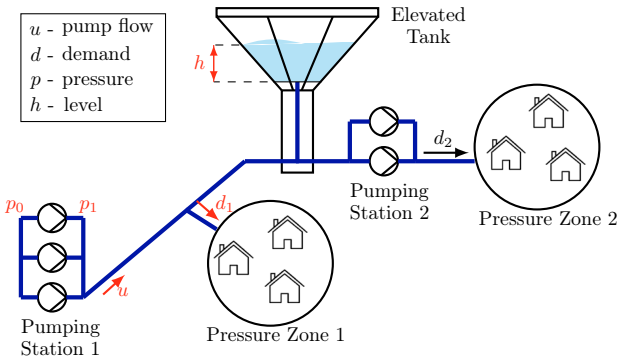

Fig. 1. Layout of a water distribution network with elevated tank and two pressure zones, where measured variables are colored with red.

Pumping station 1 (PS1) feeds the water demand to Pressure Zone 1 (PZ1) and the elevated reservoir provides the pressure in the zone. Pressure Zone 2 (PZ2) is fed directly by the elevated tank via Pumping station 2 (PS2). The dominating dynamic is due to mass conservation of water, and as such is dictated by the tank level $h(t)$, i.e.,

$$\mathcal{A}\dot{h} = u(t) - d_1(t) - d_2(t), \tag{1}$$

where $u(t)$ is the controlled flow at PS1, $d_1(t)$ is the sum of the consumption flows by the end-users in PZ1, and similarly $d_2(t)$ is the summed flow into PZ2 (depicted in Fig. 1). The surface area of the reservoir is denoted by $\mathcal{A}$. Furthermore, the consumption flows have a daily periodicity, typically with high peaks in the morning and evening hours with a small deviation between workdays and weekends. An example of demand flows from a real-world utility in Denmark is depicted in the two first plot of Fig. 4. From these data, it is clear that the variance around the moving mean is scaled with the mean consumption at any given time, i.e., high flows yield high uncertainty and visa versa. Consequently, the consumption flows for pressure zone i is well approximated with

$$d_i(t) = \bar{d}_i(t)(1 + e_i(t)) + \epsilon_i(t) \quad \forall t, \tag{2}$$

where $e_i(t) \sim \mathcal{N}(0, \sigma_{ei}^2)$, $\epsilon_i(t) \sim \mathcal{N}(0, \sigma_{\epsilon i}^2)$, and $\bar{d}_i(t)$ is the mean periodic demand flow. A flow consumption profile is defined for each pressure zone, hence $i \in \{1, 2\}$.

The pressure p_1 at PS1 depends on the level h in the tank, the flow u from PS1, and the sum of consumption flows d_1 to PZ1. In this work the pressure is approximated by

$$p_1(t) = r_1|u(t)|u(t) + r_2|u(t) - d_1(t)|\big(u(t) - d_1(t)\big) + \alpha h(t), \tag{3}$$

where α is a scaling factor between level and pressure, r_1 is the resistance term for the first part of the pipe from PS1 to the connection point to PZ1, and r_2 is the resistance term from the connection point to the elevated reservoir.

The network control needs to fulfill certain operational constraints. Firstly, overflow from the tank should be avoided. Secondly, a minimum level must be kept in the tank to ensure a safety volume, e.g., for firefighting. This leads to the following physical constraint on the water level

$$h_{\min} \leq h(t) \leq h_{\max} \quad \forall t, \tag{4}$$

where $h_{\min}$ and $h_{\max}$ are the physical bounds for the minimum and maximum tank levels, respectively. Moreover, the actuators are bounded by their physical capacity, leading to the following operational constraint on the input

$$u_{\min} \leq u(t) \leq u_{\max} \quad \forall t, \tag{5}$$

where $u_{\min}$ and $u_{\max}$ are the physically possible minimum and maximum pump flows, respectively. Finally, there are also requirements for the exchange of water in the tank, as water age degrades the stored water quality.

3. CONTROL ARCHITECTURE

We place a Global Controller (GC) on a server with IT access, executed off-site from the pumping stations, and local controllers at the pumping stations with access to sensors and actuators. This architecture provides flexibility towards changing the objectives of the optimization problem remotely and allows to access various 3rd-party services, e.g., price of energy or even CO_2 emission signals in real time. The proposed architecture is shown in Fig. 2.

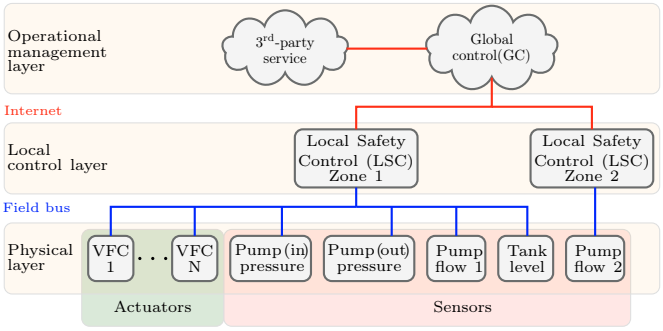

Fig. 2. Control architecture with the GC on the cloud and the LSCs on edge devices.

Water distribution networks are critical infrastructures that require undisturbed and safe operation at all times (Del Mar (2022)). To establish such safe operation, we propose to place Local Safety Controllers (LSCs) by the pumping stations. The LSCs are designed such that water supply is provided even in the case of server malfunctioning, errors in the GC, or communication breakdown. Such events may occur for instance under cyberattacks or communication breakdowns due to Distributed Denial of Service (DDoS). Moreover, man-in-the-middle attacks may manipulate the data from and to the GC-layer, leading to corrupted reference signals to the LSC. Also, unexpected operation may occur, e.g., abnormal flow due to firefighting, which is not considered explicitly in the GC-algorithm.

The physical layer consists of actuators and sensors, among which Variable Frequency Converters (VFCs) control the speed of the pumps and sensors measure the pump pressures (both inlet and outlet), the pump flows, and the level in the elevated tank. The physical layer is connected with the LSCs via a local field bus, which is assumed to be disconnected from the surroundings except through the LSC. The LSCs initiate the communication to the GC. In case of a communication request, the GC calculates the optimal flow (volume) setpoint profiles over the prediction horizon using Economic Model Predictive Control (EMPC) and communicates the entire profile $\bar{v}^*$ to the LSCs. The optimal flow profile is recalculated and communicated with a sample time ΔT, whereas the LSCs execute with a much smaller sample time $\delta t << \Delta T$, making the LSCs capable of reacting to failures in almost real time.

3.1 Global Optimal Controller

The GC placed on the cloud is designed similarly to the approach described in Kallesøe et al. (2017). The method

is an adaptive EMPC, which is designed for water distribution networks with a structure shown in Fig. 1. The internal and the disturbance model used in the EMPC scheme is found by using standard identification methods, making the approach plug-and-play. We extend the approach in Kallesøe et al. (2017) with the robust handling of the stochastic variations on end-user consumption, which leads to more cautious control behaviour. Hence, the frequency at which the LSCs intervenes is reduced, resulting in smoother flow and pressure.

The mean consumption profiles at PZ1 and PZ2 are approximated by

$$\mathbb{E}[d_1(t_k)] = \bar{d}_1(t_k) = \underbrace{\mathbb{E}[u(t_k) - \mathcal{A}(h(t_k) - h(t_k - \delta t)) - d_2(t_k))]}_{\approx g_1(t_k)},$$
$$\mathbb{E}[d_2(t_k)] = \bar{d}_2(t_k) \approx g_2(t_k), \tag{6}$$

where $g_1(t_k)$ and $g_2(t_k)$ are Fourier series, that model the mean consumption in PZ1 and PZ2, respectively.

Besides modelling the flow consumption in the network, a model describing the flow and pressure relation at the pumping stations is required. Using that $d_1(t_k) \approx g_1(t_k)$, the pressure losses in the supply line are approximated by

$$\mathbb{E}[p_1(t_k) - p_0(t_k) - \alpha h(t_k)] \approx f\big(u(t_k), g_1(t_k)\big), \tag{7}$$

where $p_0(t_k)$ and $p_1(t_k)$ are the inlet and outlet pressures of the pumping station, respectively. The function f is a parametrization of the pipe pressure drops and has a structure similar to (3). Moreover, αh is the pressure at the point where the reservoir is connected to the network.

The variance of the two models are estimated from data, given that $g_1(t_k)$ and $g_2(t_k)$ are known, i.e.,

$$\mathbb{E}[(d_i(t_k) - \bar{d}_i(t_k))^2] \approx g_i(t_k)\sigma_{ei}^2 + \sigma_{\epsilon i}^2, \quad i \in \{1, 2\} \tag{8}$$

where the right hand side has the form of a regression model, meaning that σ_{ei}^2 and $\sigma_{\epsilon i}^2$ are calculated using standard optimization methods for both pressure zones.

The fact that consumptions have a stochastic behaviour and that only the statistics of the consumption is known, implies that (1) and (2) must be reformulated to a stochastic differential equation, i.e.,

$$dh = \frac{1}{\mathcal{A}}(u(t) - \bar{d}_1(t) - \bar{d}_2(t))dt + \frac{1}{\mathcal{A}}\sum_{i=1}^{2}\left(\bar{d}_i(t)\sigma_{ei}d\beta + \sigma_{\epsilon i}d\beta\right) \tag{9}$$

where β is a standard Brownian motion. The flow planning in the GC is done with sample time ΔT. This means that the evolution of the tank level between two samples is found by integrating the stochastic differential equation (9) over the time interval t_k to $t_k + \Delta T$. Here, $i \in \{1, 2\}$ denotes the consumption of PZ1 and PZ2, respectively, and the control signal in terms of flow $u(t_k)$ is constant over the time interval. The average level at time t_{k+1} is given by (Årström, 1970, p. 51-57)

$$\bar{h}(t_{k+1}) = \mathbb{E}[h(t_{k+1})] = h(t_k) + \frac{1}{\mathcal{A}}\big(v(t_k)^* - \bar{v}_1(t_k) + \bar{v}_2(t_k)\big), \tag{10}$$

where $v(t_k)^* = \Delta T u(t_k)$ is the sampled control signal in terms of volume and $\bar{v}_1(t_k)$ and $\bar{v}_2(t_k)$ are found by solving the stochastic integral

$$\bar{v}_i(t_k) = \mathbb{E}\left[\int_{t_k}^{t_k+\Delta T} d_i(\tau)d\tau\right] \approx \int_{t_k}^{t_k+\Delta T} g_i(\tau)d\tau. \tag{11}$$

Note that the average consumption models g_i are known functions estimated by the Fourier series from past data.

The covariance of $h(t_{k+1})$ is needed for calculating the stochastic boundaries for constraining the evolution of the level in the elevated tank. The covariances are found under the assumption that the consumption flows $d_i(t_k)$ are constant and equal to the average consumptions over the sample period ΔT. That is, the consumption is $\bar{d}_i(t_k) \approx \frac{\bar{v}_i(t_k)}{\Delta T}$, where $\bar{v}_i(t_k)$ is given by (11). Hence, due to (2) the covariance is given by (Årström, 1970, p. 51-57), i.e.,

$$\mathbb{E}[(h(t_{k+1}) - \bar{h}(t_{k+1}))^2] \approx \frac{\Delta T}{\mathcal{A}}\left(\left(\frac{\bar{v}_i(t_k)}{\Delta T}\right)^2\sigma_{ei}^2 + \sigma_{\epsilon i}^2\right). \tag{12}$$

With the above model we are ready to present the optimization problem of the EMPC scheme that is to be solved at the GC level, i.e.,

$$v^* = \arg\min_{v} \sum_{k=1}^{N}\left(c(t_k)\eta\frac{v(t_k)}{\Delta T}\Delta p(t_k) + \kappa_\Delta(v(t_{k-1})) - v(t_k))^2\right) \tag{13a}$$

subject to

$$\bar{h}(t_0) = \bar{h}(t_N) \tag{13b}$$
$$\Delta T u_{\min} \le v(t_k) \le \Delta T u_{\max} \tag{13c}$$
$$\bar{h}(t_{k+1}) = \bar{h}(t_k) + \frac{1}{\mathcal{A}}\left(v(t_k) - \bar{v}_1(t_k) - \bar{v}_2(t_k)\right) \tag{13d}$$
$$\Delta p(t_k) = f\left(\frac{v(t_k)}{\Delta T}, g_1(t_k)\right) + \alpha\bar{h}(t_k) \tag{13e}$$
$$h_{\min} + \sigma_h(\bar{v}_1(t_k), \bar{v}_2(t_k)) \le \bar{h}(t_k) \le h_{\max} - \sigma_h(\bar{v}_1(t_k), \bar{v}_2(t_k)) \tag{13f}$$
$$\underline{V} < \frac{1}{2}\sum_{k=1}^{N}\left(|v(t_k) - v_1(t_k)| + v_2(t_k)\right) \tag{13g}$$

forall $k = 1, \cdots, N$. Note that $h(t_0)$ and $v^*(t_0)$ are the actual level and control signals, forming the initial conditions for the optimization problem, and $\Delta p(t_k) = p_1(t_k) - p_0(t_k)$. The first term in (13a) formulates the cost of operation, where $c(t_k)$ is a known price signal consisting of price values over the entire horizon N. The second term penalizes the rate of change of the control signal $v(t_k)$. The weight term κ_Δ is constant, and the efficiency term η is constant as well. The constraint in (13b) ensures equality between the initial tank level and the level at the end of the horizon. (13c) is a constraint on inputs, while (13d) is the dynamics, where $\bar{v}_i(t_k)$ is given by (11). The constraint in (13e) describes the pressure in the network, where $f(\cdot)$ is defined in (7). Furthermore, the constraints in (13f) ensure that the reservoir levels are within the accepted boundaries given by (4). Lastly, (13g) describes the turnover requirements of the tank ensuring water quality (Kallesøe et al. (2017)). Here, $\underline{V}$ is the minimum volume that is exchanged in the tank.

Note that the state constraints in (13f) have been extended with the tightening terms $\sigma(\bar{v}_1(t_k), \bar{v}_2(t_k))$, $k = 1, \cdots N$. Since the evolution of the system states is stochastic, we treat our state constraints as stochastic, and approximate them using chance-constraints. The tightening terms are

$$\sigma\big(\bar{v}_1(t_k), \bar{v}_2(t_k)\big) = \phi(\gamma)^{-1}\sqrt{\frac{\Delta T}{\mathcal{A}}\left(\left(\frac{\bar{v}_i(t_k)}{\Delta T}\right)^2\sigma_{ei}^2 + \sigma_{\epsilon i}^2\right)}, \tag{14}$$

where $\phi(\cdot)$ is the cumulative distribution function of the standard Gaussian distribution evaluated at γ probability level. Hence, $\mathbb{P}\big(h_{\min} \leq h(t_k)\big) \geq \gamma$ and $\mathbb{P}\big(h(t_k) \leq h_{\max}\big) \geq \gamma$. Note that the tightening in (14) can be pre-computed for the optimization problem in (13a).

Remark 1. In this work we adopt the naiive approach of chance-constrainted MPC, where the variance of the states are not predicted. Our argument is that the control effort u (with limits $u_{\min} \leq u \leq u_{\max}$) is always strong enough (the boundaries; $u_{\min}$ small enough and $u_{\max}$ large enough) to keep up with the uncertainties within each update interval ΔT. With this assumption the uncertainty is only important one-step ahead. This naiive approach leads to computation loads similar to a deterministic case, as the covariance is not propagated in time.

3.2 Local Safety Controller

The task of the LSC is two-fold. Firstly, to avoid pressure shocks in the network, the LSC must ensure smooth flow changes. Secondly, the controller has to ensure that the level constraints are fulfilled independently on the hourly volume inputs $v^*(t_k)$, communicated by the GC.

Addressing the first task, each hour the GC calculates a new volume setpoint. This setpoint is translated to a flow reference profile for the next hour corresponding to the setpoint volume. Such a flow profile is shown in Fig. 3.

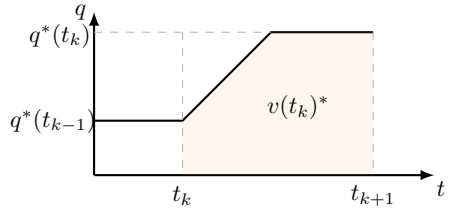

Fig. 3. Translated flow reference profile from volume communicated by the global controller.

According to Fig. 3, the flow $u^*(t_k)$ of PS1 is

$$u_l^*(t_l) = \min\{K_k(t_l - t_k),\ q^*(t_k) - q^*(t_{k-1})\} + q^*(t_{k-1}) \quad (15)$$

where k (with sample time ΔT) is the sampling index of the GC and l (with sample time δt) is the sampling index of the LSC. In (15) $q(t_k)^* = \frac{4}{3}\frac{\bar{v}(t_k)^*}{\Delta T} + \frac{1}{3}q(t_{k-1})^*$ and $K(t_k) = \frac{2(q(t_k)^* - q(t_{k-1})^*)}{\Delta T}$. Note that $q(t_k)^*, q(t_{k+1})^*, \cdots$ can be calculated recursively when $q(t_{k-1}))^*$ and $\bar{v}(t_k)^*, \bar{v}(t_{k+1})^*, \cdots$ are known. Hence, it is possible to calculate a desired control vector $\bar{u}^* = [u(t_l)^* \ \cdots \ u(t_{l+M})^*]^\intercal$ using (15).

Addressing the second task of the LSC, the volume setpoint $\bar{v}(t_k)^*$ is calculated based on the predicted consumption. The actual consumption might differ from the expected, hence the level constraint might be violated within the sample period. Such violations must be avoided with the use of the LSCs. The consumption is described by (2), where $\bar{d}_i(t_k)$ is the average daily consumption variations. The average consumption $\bar{d}_i$ is typically changing slowly, hence can be assumed to be constant over a short time. Therefore, a short-term prediction of the sum of consumptions in PZ1 and PZ2 is given by

$$d(t_{l+1}) = d(t_l) + e(t_l), \quad (16)$$

where $e(t_l) \in \mathcal{N}(0, \sigma_d^2)$. Here, σ_d describes how much the demand is expected to change between samples. Based on the short-term demand model in (16) and the discretized tank model in (1), a stochastic model is obtained

$$x(t_{l+1}) = Ax(t_l) + Bu(t_l) + e_x(t_l), \quad (17a)$$
$$y(t_l) = Cx(t_l) + e_y(t_l), \quad (17b)$$

where $x(t_l) = [d(t_l) \ v(t_l)]^\intercal$ are the short-term consumption and reservoir volumes, respectively. $u(t_l)$ is the flow delivered by PS1, and

$$A = \begin{bmatrix} 1 & 0 \\ -\delta t & 1 \end{bmatrix} \quad , \quad B = \begin{bmatrix} 0 \\ \delta t \end{bmatrix} \quad , \quad C = \begin{bmatrix} 0 & \frac{1}{\mathcal{A}} \end{bmatrix} .$$

With appropriate choices of the covariance matrices Q and R of $e_x(t_l)$ and $e_y(t_l)$ respectively, a Kalman filter is designed for estimating the state vector $\hat{x}(t_l)$. This state vector hold a short-term estimate of the consumption $\hat{d}(t_l)$, that will follow unexpected consumption changes. The estimated consumption will be used for correcting the pump flow $u(t_k)$ to avoid violating the level constraints formulated in (4). Based on $\hat{d}(t_l)$ and the flow reference $u(t_l)^*$, the actual flow that fulfills the level constraints is found by solving the optimization problem

$$\min_{\delta u} \sum_{j=0}^{M} \left(\frac{1}{2} ||u(t_{l+j}) - u(t_{l+j})^*||^2 + \kappa \frac{1}{2} ||\delta u||^2 \right) \quad (18a)$$

subject to

$$h_{\min} \leq y(t_{l+j}) \leq h_{\max} \, . \quad (18b)$$

for $j = 0, \cdots, M$, where κ is a weighting term. The corrected pump flow is then found by

$$u(t_l) = u(t_{l-1}) + \delta u. \quad (19)$$

Since the solution is aimed to solve on local edge devices, e.g., on PLCs, solving the optimization problem in (18a) numerically and online should be avoided. Hence, we seek a closed form solutions for the problem. To this end, δu is chosen to be a scalar ($\delta u \in \mathbb{R}$), meaning that we seek a ramp function that fulfills the constraints over the time horizon $m\delta t$ almost all times. Predicting the deterministic part of (17) leads to the following description of the level predictions $\bar{y} = [y(t_l) \ \cdots \ y(t_{l+m})]^\intercal$ (Maciejowski (2002)),

$$z = \Phi \hat{x}(t_{l-1}) + \Gamma \bar{u} \quad (20a)$$
$$\bar{y} = \Lambda z \, . \quad (20b)$$

where the corrected pump flows $\bar{u}$ are given by

$$\bar{u} = \mathbb{1} u(t_{l-1}) + S\mathbb{1}\delta u. \quad (21)$$

Here, $u(t_{l-1})$ is the actual flow and S is a lower diagonal matrix with ones in the lower triangle. Furthermore, using (20) in the constraints (18b) leads to the following set of constraints on δu, i.e.,

$$\mathbb{1} h_{\min} - \Lambda\Phi\hat{x}(t_{l-1}) - \Lambda\Gamma\mathbb{1}u(t_{l-1}) \leq g\delta u \quad (22a)$$

$$g\delta u \leq \mathbb{1} h_{\max} - \Lambda\Phi\hat{x}(t_{l-1}) - \Lambda\Gamma\mathbb{1}u(t_{l-1}), \quad (22b)$$

where $g = \Lambda\Gamma S\mathbb{1}$ is a vector. Hence each row of (22a) and (22b) can be evaluated individually. In the following let $G = \text{diag}\{g\}$ such that $g = G\mathbb{1}$.

The constrains (22a) and (22b) cannot be fulfilled for any values of $u(t_{l-1})$ and $x(t_{l-1})$. However, the upper constraints (22b) have priority since violating these constraints can lead to reservoir overflows and potential damages to the surroundings. These upper constraints can always be fulfilled by a proper choice of δu for any $x(t_{l-1})$ and $u(t_{l-1})$.

In the following, we will use the projection method described in Bertsekas (1976) to solve the constrained optimization problem. Projections are particularly easy in $\mathbb{R}$, hence the formulation of the optimization problem. The solution to the optimization problem is given by

$$0 = \mathbb{1}^T S^T(\mathbb{1}u(t_{i-1}) - \bar{u}^* + S\mathbb{1}\delta u) + \kappa\mathbb{1}^T\mathbb{1}\delta u \quad \Leftrightarrow$$
$$\delta u = (\mathbb{1}^T S^T S\mathbb{1} + \kappa\mathbb{1}^T\mathbb{1})^{-1}(\mathbb{1}^T S^T\bar{u}^* - \mathbb{1}^T S^T\mathbb{1}u(t_{i-1})). \quad (23)$$

The solution must be projected onto the feasible region defined by (22a) and (22b) with priority to (22b). Alg. 1 solves the LSC optimization problem (18) for each t_l.

Algorithm 1 Local safety controller.

Require: Settings: $h_{\max}$, $h_{\min}$, κ, $\mathcal{A}$.
  for each sample time t_l **do**
    Predict control values $\bar{u}^*$ using (15).
    Sample values u_{l-1}, h_l.
    Update the Kalman filter to obtain $\hat{x}_l$.
    Calculate optimal flow step using (23).
    Project into the feasible region using:
    if $\delta u \leq \max G^{-1}(\mathbb{1}h_{\min} - \Lambda\Phi\hat{x}_{l-1} - \Lambda\Gamma\mathbb{1}u_{l-1})$ **then**
      $\delta u \leftarrow \max G^{-1}(\mathbb{1}h_{\min} - \Lambda\Phi\hat{x}_{l-1} - \Lambda\Gamma\mathbb{1}u_{l-1})$.
    end if
    if $\min G^{-1}(\mathbb{1}h_{\max} - \Lambda\Phi\hat{x}_{l-1} - \Lambda\Gamma\mathbb{1}u_{l-1}) \leq \delta u$ **then**
      $\delta u \leftarrow \min G^{-1}(\mathbb{1}h_{\max} - \Lambda\Phi\hat{x}_{l-1} - \Lambda\Gamma\mathbb{1}u_{l-1})$.
    end if
    Update the pump flow: $u_l \leftarrow u_{l-1} + \delta u$.
  end for

where the settings are only accessible from the local device.

4. NUMERICAL RESULTS

In the following, we test the proposed control architecture in a simulation environment where a water distribution network with a structure similar to the one shown in Fig. 1 is utilized. The parameters and consumption profiles are from a small water utility in the city Bjerringbro, Denmark. The parameters describing the network are $\mathcal{A} = 240[\text{m}^2]$, $r_1 = r_2 = 5$ $[\text{m}/(\text{m}^3/\text{h})^2]$, and $\alpha = 1[\text{mWc}/\text{m}]$. In the following test results, the weight of the EMPC (13) is $\kappa_\Delta = 100$, found by trial-and-error. The prediction horizon is $N = 24$ with a sample time $\Delta T = 1[\text{hour}]$. The sample time of the local control $\delta t = 1[\text{min}]$ with a prediction horizon $M = 15$ steps. For the tests, we define three failure scenarios relevant for water systems, i.e.,

Event 1: Abnormal water consumption in PZ1 caused by, e.g. fire fighting or pipe burst.
Event 2: Hacking of the GC algorithm, forcing a flow reference to make the elevated reservoir overflow.
Event 3: Communication breakdown between the GC and LSC controllers, caused by, e.g. network failures, DDoS attacks, or breakdown of the cloud server.

The results are shown in Fig. 4, where (a) and (b) show the measured and predicted consumption in PZ1 and PZ2, respectively. Fig. 4(c) compares the actual and the predicted water levels in the tank, whereas Fig. 4(d) shows the pumped flow at PS1, along with the occasions where the LSC overrules the GC flow setpoints. Finally, Fig. 4(e) shows the electricity prices for the given period. The tests are conducted with consumption profiles for PZ1 and PZ2 in the period from Jan 01 to Jan 10 in 2022, and historical electricity price data [1] from the same period. Our aim is to show that the failures do not affect the operation of the water network, hence the proposed control architecture is robust and safe.

Event 1 shows the first failure scenario, where a 50 $[m^3/h]$ increase in consumption is introduced in PZ1 from Jan 02 02:00 to 10:00. From Fig. 4(c) it is evident that the increased consumption empties the tank and the LSC overrules the flow setpoint to avoid violating the level constraint. Shortly after, the EMPC algorithm placed on the GC layer can handle the increased consumption and the level is continued to be within the constrained levels. Due to the continuous update of the consumption predictions, the abnormal flow event is saved in the telemetry, hence the EMPC over-predicts the consumption the following day and the uncertainty increases significantly in both Fig. 4(a) and Fig. 4(c). Note that the incorrect prediction does affect the control in a short period after the event, but not to the degree that the LSC needs to intervene.

Event 2 shows the second failure scenario, where a cyber-attack is simulated from Jan 05 00:00 to 14:00. It is anticipated that a hacker manipulates the flow reference calculated by the GC and overwrites it to the highest possible flow setpoint to cause overflow. As seen in Fig. 4(c) and Fig. 4(d), when the level reaches the maximum bound, the LSC activates and reduces the flow setpoint. The activation keeps the water level at its maximum, but not above. In Fig. 4(d), the red crosses indicate that the LSC is active during the entire cyber-attack and it is clear that the flow reference 80 $[m^3/h]$ dictated by the GC (red line) is reduced by the LSC (blue line).

Event 3 imposes a scenario where a communication error is introduced from Jan 08 00:00 to 18:00. During the failure, the LSC continues the system operation with the latest set of optimal reference points calculated and transmitted from the GC. As seen in Fig. 4(c), the latest setpoints are accurate enough to keep the water level within the constraints almost at all times. From Fig. 4(d), it is evident that the LSC is only activated when the water level hits the upper level bound, meaning that the flow is reduced.

5. CONCLUSION

This paper investigated a control architecture that enables an integrated IT/OT setup to utilize fluctuating electricity prices in economic predictive control for water distribution networks. From an operation and implementation point of view, it comes naturally to place the predictive control algorithm on a cloud server, thereby having the possibility for connectivity and access to third-party market prices of electricity. However, proposing such architecture raises cyber-security risks. The proposed control methods and architecture mitigate this risk by introducing a local safety controller. The robustness of the proposed methods is tested numerically on a real-world network structure and with real data provided by the utility in Bjerringbro, Denmark. The numerical tests verifies the robustness to different unanticipated events, such as abnormal flow, cyber-attacks, and communication errors. Moreover, as

[1] The historical electricity market data is obtained with Energinet's DataHub, accessed at https://www.energidataservice.dk/tso-electricity/Elspotprices.

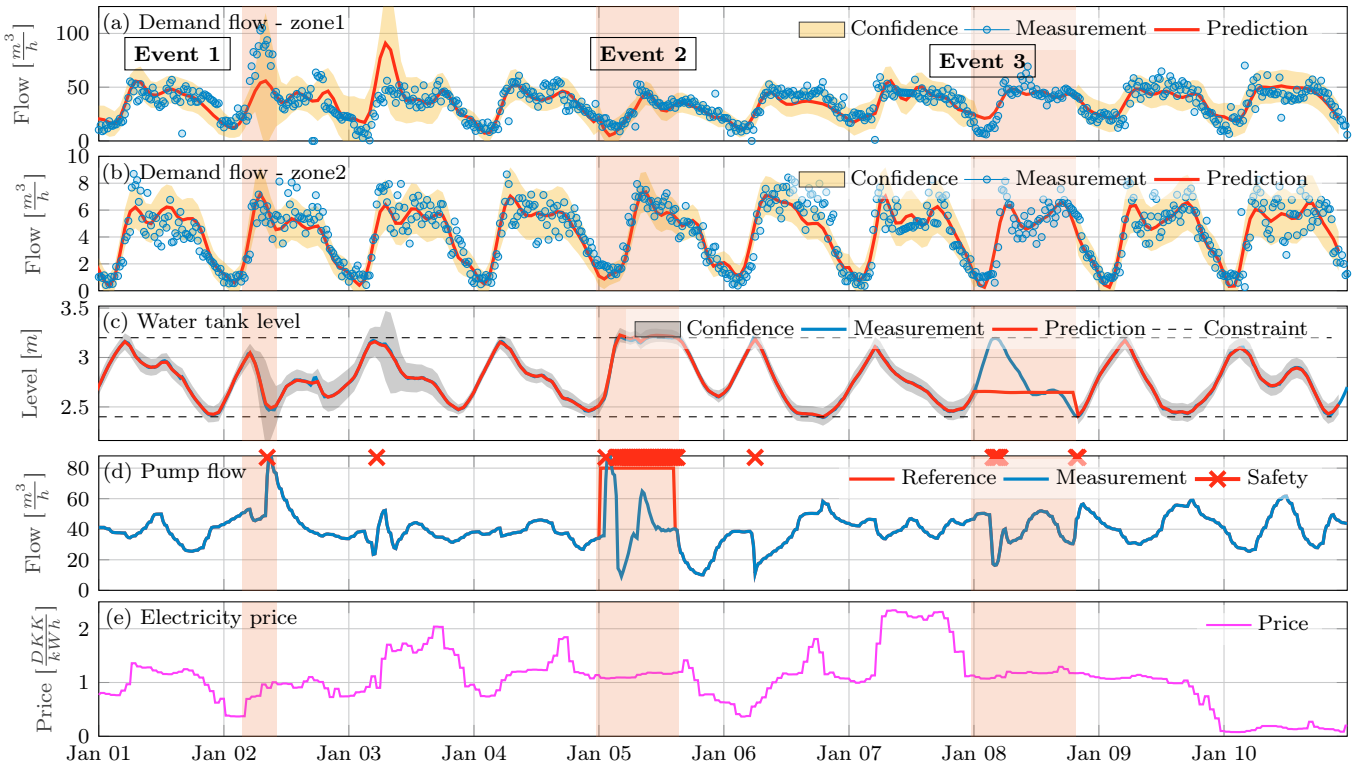

Fig. 4. Test results over a 10-days period of operation, where the different failure scenarios are tested (shaded with red).

the EMPC is adaptive, the control adapts to changes in consumption over the year.

ACKNOWLEDGEMENTS

The authors would like to thank the utility in Bjerringbro, Denmark for letting us use their data for this research.

REFERENCES

Bertsekas, D.P. (1976). On the goldstein - levitin - polyak gradient projection method. *IEEE Trans. on Automatic Control*, 21, 174–184.

Cembrano, G., Wells, G., Quevedo, J., Perez, R., and Argelaguet, R. (2000). Optimal control of a water distribution network in a supervisory control system. *Control Engineering Practice*, 8, 1177–1188.

Corte, A.D. and Sörensen, K. (2013). Optimisation of gravity-fed water distribution network design: A critical review. *European Journal of Operational Research*, 228, 1–10.

Del Mar, N.A.M. (2022). The nis2 directive: A high common level of cybersecurity in the eu.

Douglas, H.C., Taormina, R., and Galelli, S. (2019). Pressure-driven modeling of cyber-physical attacks on water distribution systems. *Journal of Water Resources Planning and Management*, 145(3), 06019001.

ENTSO (2022). Central collection and publication of electricity generation, transportation and consumption data and information for the pan-european market. URL `https://transparency.entsoe.eu/`.

Escudero, C., Sicard, F., and Zamai, E. (2018). Process-aware model based idss for industrial control systems cybersecurity: Approaches, limits and further research. In *IEEE 23rd International Conf. on Emerging Technologies and Factory Automation (ETFA)*. Torino, Italy.

International Energy Agency, I. (2022). World energy outlook 2022.

Kallesøe, C.S., Jensen, T.N., and Bendtsen, J.D. (2017). Plug-and-play model predictive control for water supply networks with storage. *IFAC-PapersOnLine*, 50(1), 6582–6587.

Maciejowski, J.M. (ed.) (2002). *Predictive Control with Constraints*. Prentice Hall.

Ocampo-Martinez, C., Puig, V., Cembrano, G., and Quevedo, J. (2013). Application of predictive control strategies to the management of complex networks in the urban water cycle. *IEEE Control Systems Magazine*, 33, 15–41.

Rao, V.M. and Francis, R.A. (2015). Critical review of cybersecurity protection procedures and practice in water distribution systems. In *Industrial and Systems Engineering Research Conf.* Nashville, Tennessee, USA.

Taormina, R., Galelli, S., Douglas, H., Tippenhauer, N.O., Salomons, E., and Ostfeld, A. (2019). A toolbox for assessing the impacts of cyber-physical attacks on water distribution systems. *Environmental modelling & software*, 112, 46–51.

Trnka, P., Pekař, J., and Havlena, V. (2011). Application of distributed mpc to barcelona water distribution network. In *18th IFAC World Congress*. Milano, Italy.

Val, J., Wisniewski, R., and Kallesøe, C.S. (2021). Safe reinforcement learning control for water distribution networks. In *IEEE Conf. on Control Systems and Technology (CCTA)*. San Diego, California, USA.

Wang, Y., Puig, V., and Cembrano, G. (2017). Non-linear economic model predictive control of water distribution networks. *Journal of Process Control*, 56, 23–34.

Årström, K.J. (ed.) (1970). *Introduction to Stochastic Control Theory*. Dover Publications.